The Impact of Atmosphere on the Local Luminescence Properties of Metal Halide Perovskite Grains

Roberto Brenes, Christopher Eames, Vladimir Bulović, M. Saiful Islam, and Samuel D. Stranks*

Metal halide perovskites are exceptional candidates for inexpensive yet high-performing optoelectronic devices. Nevertheless, polycrystalline perovskite films are still limited by nonradiative losses due to charge carrier trap states that can be affected by illumination. Here, in situ microphotoluminescence measurements are used to elucidate the impact of light-soaking individual methylammonium lead iodide grains in high-quality polycrystalline films while immersing them with different atmospheric environments. It is shown that emission from each grain depends sensitively on both the environment and the nature of the specific grain, i.e., whether it shows good (bright grain) or poor (dark grain) luminescence properties. It is found that the dark grains show substantial rises in emission, while the bright grain emission is steady when illuminated in the presence of oxygen and/or water molecules. The results are explained using density functional theory calculations, which reveal strong adsorption energies of the molecules to the perovskite surfaces. It is also found that oxygen molecules bind particularly strongly to surface iodide vacancies which, in the presence of photoexcited electrons, lead to efficient passivation of the carrier trap states that arise from these vacancies. The work reveals a unique insight into the nature of nonradiative decay and the impact of atmospheric passivation on the microscale properties of perovskite films.

Metal halide perovskites have ushered in a paradigm shift for optoelectronics, with the potential to fabricate solar photovoltaics (PV) and light-emission devices which are both high performance and inexpensive.[1] One unique feature is their remarkable tolerance to defects, allowing thin films to be fabricated by relatively crude solution-processing methods while still achieving high crystallinity,[2] strong absorption,[3] and long charge carrier diffusion lengths.[4] Although recent mixed-cation, mixed-halide alloyed configurations have shown enhanced stability and performance, methylammonium lead iodide (MAPbI$_3$) represents the archetypical perovskite system for understanding material and optoelectronic behavior.[5] Perovskite-based PV devices on small laboratory prototype scales have demonstrated power conversion efficiencies (PCEs) exceeding 22%,[6] which is approaching those of established thin-film technologies. Light-emitting diodes (LEDs) have shown external quantum efficiencies between 8% and 12% over several emission colors,[7] and lasing properties have also been demonstrated.[8]

Nevertheless, despite impressive progress, the performance of these perovskite films is still limited. For instance, the photoluminescence quantum efficiency (PLQE) of thin films corresponding to high device performances is still far from unity, with typical measured values on the order of ≈1%–10% at excitation intensities equivalent to solar illumination.[9] This is consistent with a sizeable density of subgap trap states that act as nonradiative recombination centers but can be filled with charge carriers at higher intensities.[10–12] These trap states are distributed heterogeneously on the microscale[13] leading to a grain-to-grain heterogeneity in optoelectronic properties, such as photoluminescence (PL),[14] photocurrent, and photovoltage.[15,16] In order for a PV or LED to reach its theoretical performance limits, recombination should be entirely radiative with all nonradiative recombination eliminated.[17] A thorough understanding of what factors influence the nonradiative decay pathways (i.e., what makes a "dark" grain poorly luminescent), as well as elucidating ways to remove these unwanted phenomena, will be critical to taking this technology toward commercialization.

Recently, we and others demonstrated that light-soaking films could lead to reductions in trap density and enhancements in luminescence properties.[11,18–21] These enhancements correlated with a photoinduced migration of iodide species away from the illuminated region, suggesting that the
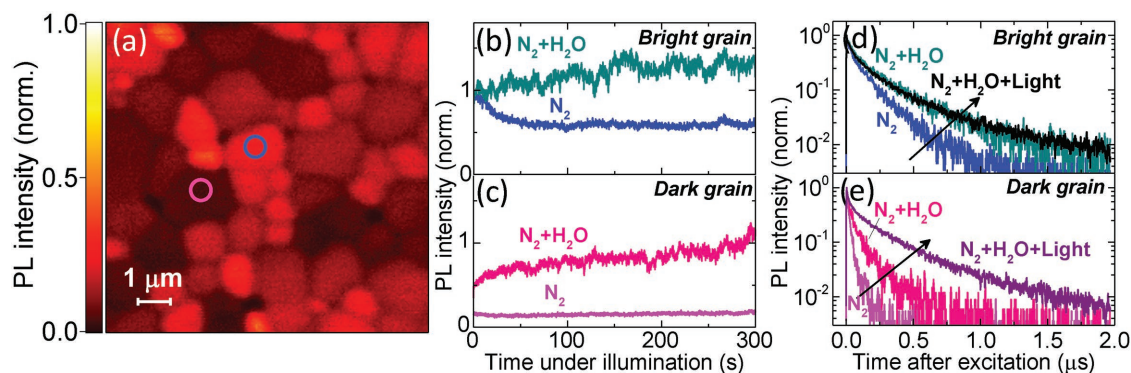
R. Brenes, Prof. V. Bulović, Dr. S. D. Stranks
Research Laboratory of Electronics
Massachusetts Institute of Technology
77 Massachusetts Avenue, Cambridge, MA 02139, USA
E-mail: sds65@cam.ac.uk
Dr. C. Eames, Prof. M. S. Islam
Department of Chemistry
University of Bath
Bath BA2 7AY, UK
Dr. S. D. Stranks
Cavendish Laboratory
JJ Thomson Avenue, Cambridge CB3 0HE, UK

The ORCID identification number(s) for the author(s) of this article can be found under https://doi.org/10.1002/adma.201706208.

**ADVANCED
SCIENCE NEWS**

www.advancedsciencenews.com
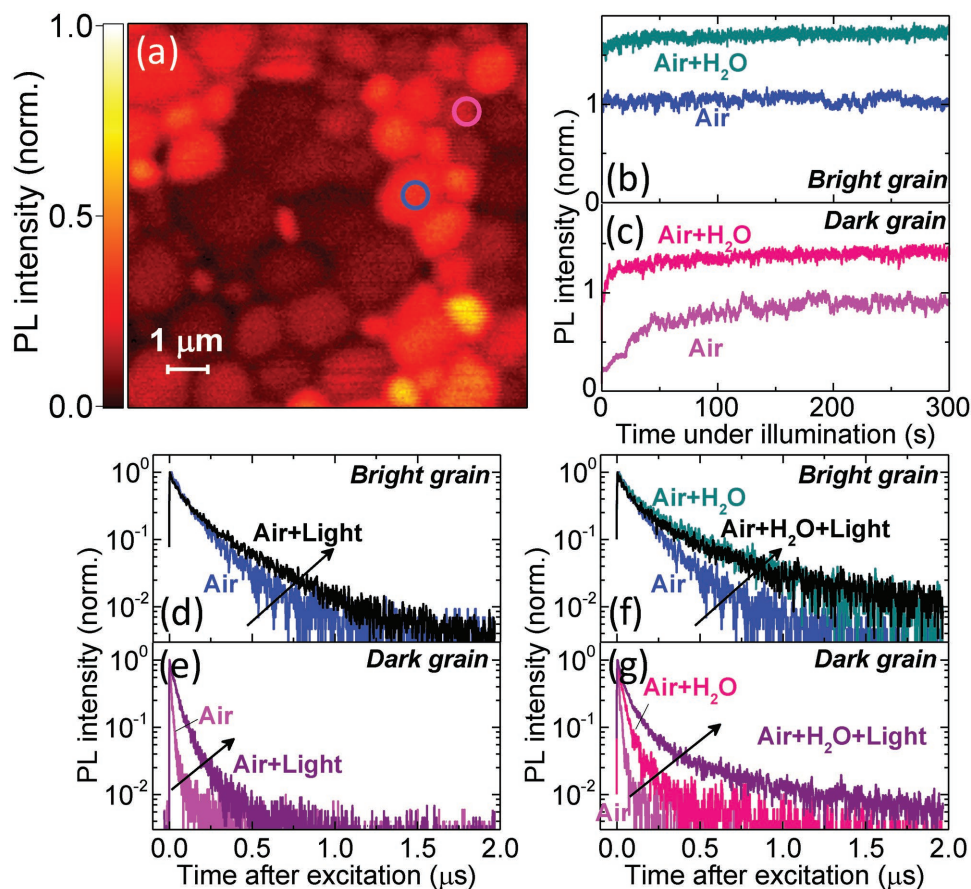
**ADVANCED
MATERIALS**

www.advmat.de

Figure 1. Microscale photoluminescence properties in dry and humid nitrogen. a) Confocal PL map of a MAPbI$_3$ perovskite film in dry nitrogen normalized to the maximum intensity. b,c) Monitoring the PL intensity (emission count rate) over time under illumination from b) a bright grain (blue circle in (a)) and c) a dark grain (pink circle in (a)) under dry nitrogen and under humidified ($\approx$45% relative humidity) nitrogen. The PL intensity for each trace over time is given relative to the starting value for the bright grain in nitrogen, which is normalized to 1. d,e) PL decays from the same d) bright and e) dark grains under dry nitrogen, and before and after light soaking in humidified nitrogen. Samples were photoexcited with a 405 nm laser with a repetition rate of 0.5 MHz and a fluence of $\approx$1 μJ cm^{-2} per pulse ($\approx$500 mW cm^{-2}), and this same laser was used for local light soaking (total photon dose of $\approx$150 J cm^{-2}).

traps are related to halide species and/or their corresponding vacancies.[22] Tian et al.[19] and Galisteo-Lopez et al.[23] recently reported that the photobrightening effects were further enhanced in the presence of oxygen. Other groups reported that exposure of the films to moisture during preparation or through a post-treatment was crucial in obtaining reasonable luminescence and device performance.[24,25] Our recent work showed that particular combinations of wide-area light soaking with atmospheric exposure could lead to remarkably high macroscopic internal PLQE values which approach 100%.[21] These results are consistent with recent reports on perovskite single crystals in which the surface photoluminescence properties were shown to be modulated by the adsorption of oxygen and water molecules.[26,27] In other work, oxygen has been reported to be detrimental to the photoluminescence properties and also the device and material stability, particularly with exposure over hours to days in the presence of light.[28,29] Likewise, moisture is known to be detrimental to perovskite stability by acting on the highly hygroscopic organic cation (e.g., methylammonium).[30] Finally, some reports have found that light exposure actually decreases the PL of the film.[31] Many of these results are conflicting and the community has not yet reached a consensus on the impact that light, in conjunction with each specific environment, has on the optoelectronic properties. It will be particularly crucial to understand these phenomena on the microscale level, a length scale in which we see substantial local luminescence losses that must be eliminated.

In this work, we explore the impact of light-soaking individual MAPbI$_3$ grains in polycrystalline films while immersing them with different atmospheric treatments. We use in situ micro-PL measurements to show that the response of each grain to continuous illumination depends sensitively on both the atmospheric environment and the nature of the specific grain, i.e., whether it shows good (bright grain) or poor (dark grain) luminescence properties. We find that both bright and dark grains show a small decrease in emission intensity under illumination over time in dry nitrogen. If they are instead illuminated in the presence of oxygen or moisture, the emission from the more defect-rich dark grain rises substantially, while

the emission from the less-defective bright grain is constant. For the synergistic combination of illumination during exposure to both air and humidity, the properties of the dark grains approach those of the bright grains, leading to extremely stable and highly luminescent grains. We explain our results using density functional theory (DFT) calculations to compute the adsorption energies of each molecule on the perovskite surfaces. We find that oxygen molecules bind particularly strongly to iodide vacancies which, in the presence of photoexcited electrons, lead to passivation of the carrier trap states that arise from these vacancies. Our work resolves the seemingly conflicting literature to date and reveals the strong influence of atmospheric molecules on the perovskite emission properties.

High-quality thin films ($\approx$250 nm thickness) of MAPbI$_3$ perovskite were deposited on cover slip glass by spin coating a lead-acetate-based precursor solution containing a hypophosporous acid additive, followed by annealing of the films (see Experimental Section).[32] A confocal PL map of the resulting film measured under dry nitrogen is shown in **Figure 1**a, clearly showing the grain-to-grain heterogeneity in emission. In a nitrogen atmosphere, we light soak the grains highlighted with the circles in Figure 1a over 5 min (total photon dose of $\approx$150 J cm^{-2} for all measurements herein), and we show the PL count rate over time under illumination in Figure 1b for a bright grain (blue circle in panel a) and in Figure 1c for a dark grain (pink circle in panel a). Under dry nitrogen, both bright and dark grains show an initial drop in emission over several minutes that eventually stabilize at a lower PL level and slowly rise over longer periods. There is a negligible change in local lifetime for these grains light soaked in dry nitrogen (Figure S1, Supporting Information). When the sample is now exposed in situ to humidified nitrogen ($\approx$45% relative humidity), we see strikingly different behavior. The bright grain now shows a rise over time under illumination, while the baseline level of the dark grain increases in the presence of moisture ($\approx$2 $\times$ the initial value) and also continues to rise over time under illumination. We show the local PL decays of the same grains in Figure 1d,e. The lifetime of the bright grain (Figure 1d) increases after exposure to humidified nitrogen but does not substantially change

Figure 2. Microscale photoluminescence properties in dry and humid air. a) Confocal PL map of a MAPbI$_3$ perovskite film in dry air normalized to the maximum intensity. b,c) Monitoring the emission (PL count rate) over time under illumination from: b) a bright grain (blue circle in (a)) and c) dark grain (pink circle in (a)) under dry air and under humidified (≈45% relative humidity) air. The PL intensity for each trace over time is given relative to the starting value for the bright grain in air, which is normalized to 1. d,e) PL decays from the same d) bright and e) dark grains under dry air before and after the light soaking. f,g) PL decays from the same bright (f) and dark (g) grains under dry air, humidified air, and after the light soaking in humidified air. Samples were photoexcited with a 405 nm laser with a repetition rate of 0.5 MHz and a fluence of ≈1 μJ cm^{-2} per pulse (≈500 mW cm^{-2}), and this same laser was used for local light soaking (total photon dose of ≈150 J cm^{-2}).

after additional light soaking. The dark grain (Figure 1e) has a very short initial lifetime, which is increased upon exposure to humidity and further increased with light soaking, with the final lifetime approaching that of the bright grain. The net effect of light soaking in humidity is that the dark and bright grains reach similar intensities and lifetimes. We note that the increase in both local PL lifetime and local PL intensity is consistent with reduced nonradiative recombination in that local area.[33]

In **Figure 2**, we show the same measurements but now performed in the presence of oxygen molecules (compressed air) instead of pure nitrogen. In the case of dry air, we now find that bright grain exhibits stable PL over time (Figure 2b), while the dark grain, which likely has a higher defect density than the bright grain, shows significant PL enhancement under illumination and eventually reaches the same intensity as the bright grain (Figure 2c). This is also reflected in the larger increase in the PL lifetime following the illumination dose for the dark grain (Figure 2e) than for the bright grain (Figure 2d). Upon introducing water molecules to the system (≈45% relative humidity), we see an initial baseline increase (i.e., before any light

soaking) in the emission intensity for both bright (Figure 2b) and dark (Figure 2c) grains. By contrast, we note that a baseline increase in the dark in dry air conditions is only observed when the samples are stored in compressed air for periods of hours (Figure S2, Supporting Information), suggesting that the impact of oxygen molecules in the dark is much more slowly acting than water molecules in the dark. The emission from both bright and dark grains in humid air then slowly rises over time under illumination, again with a greater relative increase for the dark grain than the bright grain. The local PL lifetimes for the bright grain (Figure 2f) increase upon humidity exposure but then do not substantially increase further under illumination, while the dark grain (Figure 2g) shows an additional increase after illumination. These collective observations highlight that the presence of molecules, such as oxygen or moisture, is vital for substantial net PL enhancement of grains under illumination, and that the presence of both oxygen and moisture under light is synergistic.[21] In contrast, illumination in a nitrogen environment without any other atmospheric (oxygen or humidity) exposure during processing or as a posttreatment leads to net decreases in emission (cf. Figure 1). We

ADVANCED
SCIENCE NEWS
www.advancedsciencenews.com

ADVANCED
MATERIALS
www.advmat.de
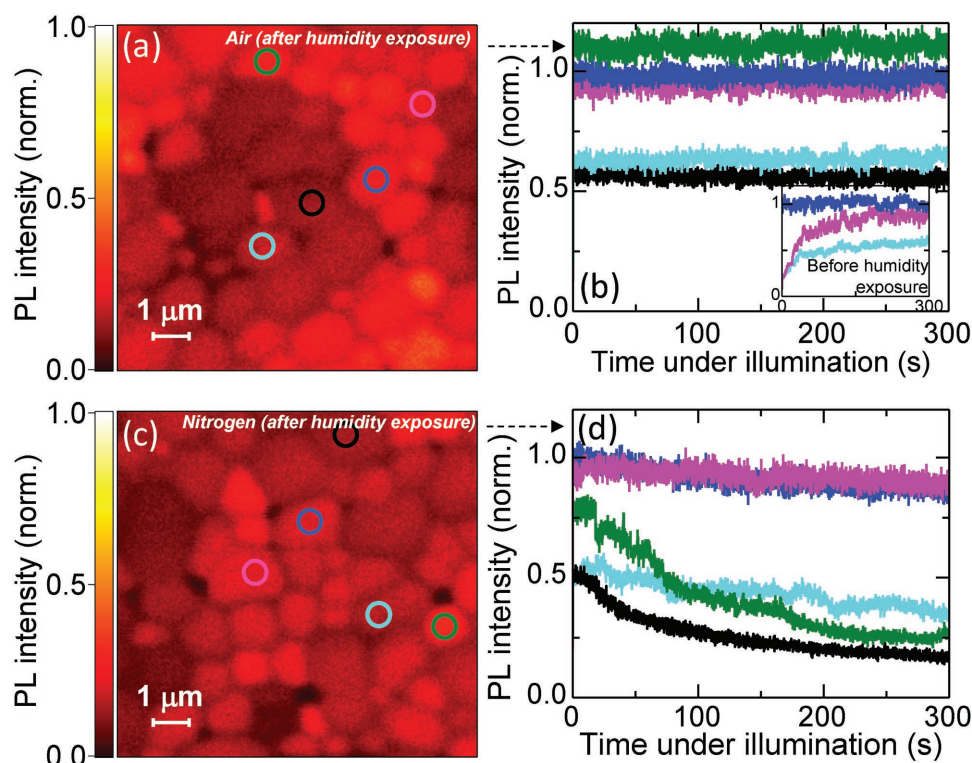
Figure 3. Local grain emission stability after humidity exposure. a) Confocal PL map of a MAPbI$_3$ perovskite film in dry air following exposure to humid air for 60 min, normalized to the same intensity value as Figure 2a to allow direct comparison. b) Monitoring the emission intensity (count rate) from various bright and dark grains denoted in (a) over time under illumination, normalized to the intensity of the same grain as in Figure 2b. Inset: emission from the same grains under continuous illumination before the exposure to humidity. c) Confocal PL map of a MAPbI$_3$ perovskite film in dry nitrogen following exposure to humid nitrogen for 60 min, normalized to the same intensity value as Figure 1a. d) Monitoring the emission intensity (count rate) from various bright and dark grains denoted in (c) over time under illumination, normalized to the intensity of the same grain as in Figure 1b. Samples were photoexcited with a 405 nm laser with a repetition rate of 0.5 MHz and a fluence of ≈1 μJ cm^{-2} per pulse (≈500 mW cm^{-2}), and this same laser was used for local light soaking (total photon dose of ≈150 J cm^{-2}).

note that the PL intensity drops even more substantially and continually under light in vacuo (i.e., in the absence of any atmospheric molecules, Figure S3, Supporting Information). We also note here that these enhancements are seen after just brief exposure to oxygen, humidity, and light (on order 10 min), but longer term exposure to oxygen, humidity, and light (on order of hours to days) leads to degradation.[21,28,29] We also reiterate that such significant enhancements require illumination of either local grains or many grains, highlighting the key role of light in these brightening processes.[18,21]

In **Figure 3**a, we show the confocal PL map of the same sample as in Figure 2a but now after exposure to humid air (45% relative humidity) for 60 min and then returning to dry air, revealing an increase in the baseline PL intensity and more uniform emission distribution compared to before the humidity exposure.[21,25] Remarkably, we find that individual grains now show exceptional PL stability after this exposure, regardless of whether they were dark or bright or previously illuminated or not (Figure 3b; grain highlighted by green circle was not previously light soaked). This can be compared to the PL of the same grains before the humidity exposure in which the darker grains in particular exhibit slow transient rises under illumination (Figure 3b inset and Figure S4, Supporting Information). By contrast, this same PL stability is

not observed when the humidity exposure is performed in nitrogen rather than air (Figure 3c,d). This suggests that the combination of both air and humidity is essential for attaining exceptional grain luminescence stability, where the introduction of humidity in general leads to less reversible effects.[21] We note that the absolute emission intensity is also increased if exposed to light during the humidity exposure (cf. Figures 1 and 2). We also note that the grains are not always stable while light soaking in humid air conditions, though after drying the system even these grains retain excellent stability (Figure S5, Supporting Information).

In order to understand these PL observations at the atomic scale, we performed DFT calculations involving the adsorption of N$_2$, O$_2$, and H$_2$O molecules onto the (110) and (001) surfaces of MAPbI$_3$. Previous studies on MAPbI$_3$ surfaces have examined the (001) and (110) surface structures[34,35] with recent atomic-scale structural and simulation studies on molecular interactions at perovskite halide surfaces.[36,37] Ab initio simulation work of Zhang and Sit[38] considered the role of excess electrons and oxygen in the degradation of MAPbI$_3$ with the creation of superoxide species which react with the (110) surface to form Pb—O bonds. However, there is currently no report of a systematic comparison of the adsorption energetics and surface electronic structures for O$_2$, N$_2$, and H$_2$O on MAPbI$_3$ surfaces.

Table 1. Adsorption energies of N_2, H_2O, and O_2 molecules onto iodine vacancies on a PbI_2-terminated (110) surface of $MAPbI_3$, with the vacancy in three possible charge states due to photoexcitation. See Table S1 (Supporting Information) for adsorption energies for binding to Pb^{2+} on the PbI_2-terminated surface and Table S2 (Supporting Information) for the (001) configuration.

| Adsorbate	Surface site	Charge state	Adsorption energy [eV]
N_2	V_I'	−1	−0.12
	$V_I^\times$	0	−0.14
	$V_I^{\cdot}$	+1	−0.15
H_2O	V_I'	−1	−0.66
	$V_I^\times$	0	−0.46
	$V_I^{\cdot}$	+1	−0.54
O_2	V_I'	−1	−3.94
	$V_I^\times$	0	−2.48
	$V_I^{\cdot}$	+1	−0.72

To simulate the effect of illuminated and dark conditions, we allowed each surface to have three charge states: positively charged, negatively charged, and neutral (dark conditions, no photoexcitation). Since it is well known that the surface regions of $MAPbI_3$ can contain high numbers of iodine vacancies,[34] we have considered both defect-free (PbI_2-terminated) and iodine-vacancy-rich surface terminations. We note that the absolute halide vacancy concentration will be higher in the illuminated case due to photoinduced halide migration away from the illuminated surface.[18]

In **Table 1**, we summarize the molecular adsorption energies for N_2, O_2, and H_2O onto an iodine vacancy on a PbI_2-terminated (110) surface of $MAPbI_3$ (see Table S1, Supporting Information, for adsorption energies for binding to Pb^{2+} on the PbI_2-terminated surface and Table S2, Supporting Information, for the (001) configuration). The adsorption energy is relative to the reference situation of infinite separation between the surface and molecule; a negative value indicates a favorable interaction. Three general features are readily apparent from this data. First,

the adsorption energies for nitrogen are around −0.15 eV and suggest physisorption, in which the interaction with the surface is relatively weak (absolute value typically less than 0.3 eV);[39] here, we find that there is no significant bond formation between the N_2 molecule and perovskite surface. Second, adsorption of H_2O is slightly more favorable, with adsorption energies in the range of −0.46 to −0.66 eV, in good agreement with other computational work[37] and suggesting weak chemisorption including hydrogen bonding. Finally, we find strong adsorption energies (absolute value >1.3 eV) for O_2 on surfaces where excess electrons are available, such as negatively charged surfaces or those with neutral iodine vacancies. O_2 adsorption onto iodine vacancies where electrons are available is the most favorable (−3.94 eV). This suggests strong chemisorption of O_2 at $MAPbI_3$ surfaces in which O_2 acts as an electron scavenger; this is associated with a favorable electron transfer process at the perovskite surface to form superoxide (O_2^-) species. Indeed, a lengthening of the O_2 bond is found, which is indicative of superoxide (O_2^-) formation. Although there are currently no experimental energies for direct comparison, the magnitude of our values is highly consistent with data found for the physisorption and chemisorption of simple molecules on solid surfaces.[40]

Given these adsorption energy results, we then calculated the surface band structure to examine the effect of adsorption on the electronic structure, and these results are summarized for the (110) configuration in **Figure 4** (see Figures S6–S9, Supporting Information for all (110) results and Figures S10–S15 (Supporting Information) for the (001) results). We define trap states as electronic states with energies greater than kT (≈25 meV) below the Fermi level, which can act to effectively localize charge[41] and trap the carriers, leading to nonradiative decay pathways.[9,12] Previous computational work on defects in $MAPbI_3$[34,42] has found that the iodine vacancy induces electron and hole trapping levels inside the bandgap region.

For the defect-free surface in the dark, there are few trap states near the bottom of the conduction band (Figure 4a). For a surface containing a high concentration of iodide vacancies and
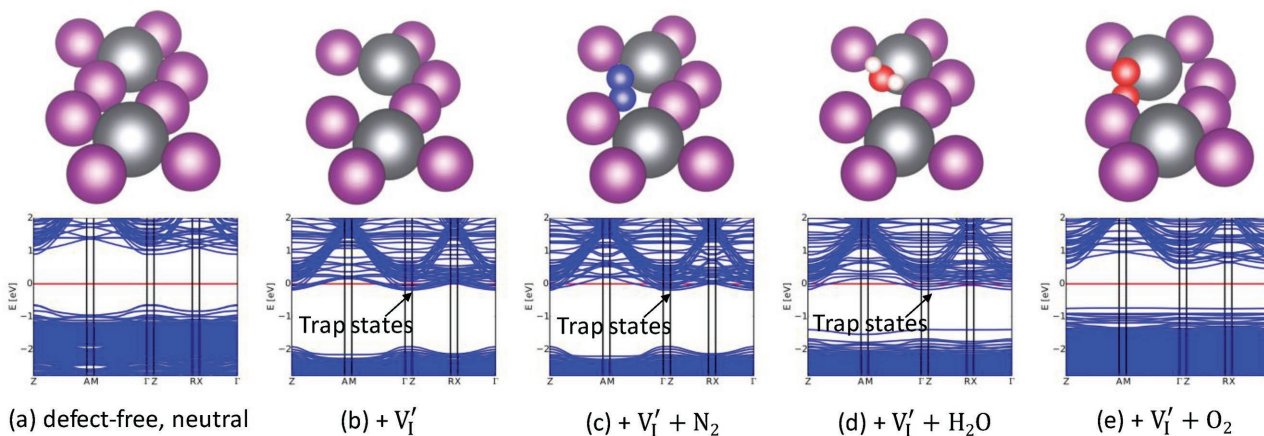
Figure 4. Surface atomic and electronic structures. Schematic representation of the local atomic-scale configurations of the surface termination layer (top row) and calculated band structures (bottom row) for the (110) surface of $MAPbI_3$. a) Pristine uncharged surface, b) negatively charged iodine vacancy into which the following molecules are adsorbed; c) N_2, d) H_2O, and e) O_2. Key: purple–iodine, gray–lead, blue–nitrogen, red–oxygen, and white–hydrogen. We note that our calculations explicitly included excess electrons; hence, the Fermi level (red line) is above any trap states because those states are filled (see Figures S6–S9, Supporting Information for other configurations).

(a) defect-free, neutral
(b) + V_I'
(c) + V_I' + N_2
(d) + V_I' + H_2O
(e) + V_I' + O_2

**ADVANCED
SCIENCE NEWS**

www.advancedsciencenews.com

**ADVANCED
MATERIALS**

www.advmat.de

with excess electrons (Figure 4b), our calculations indicate trap states at the bottom of the conduction band, evidenced by their occupancy in the presence of excess electrons and the shift of the Fermi level (red line) into the conduction band. When N_2 or H_2O is adsorbed there is very little change in the surface band structure (Figure 4c,d). In contrast, when O_2 is adsorbed there is a large reduction in the number of trap states, which shift down to the top of the valence band (Figure 4e), indicative of chemisorption. In recent work,[29] we have shown that this is due to the O_2 becoming reduced to a superoxide ion (O_2^-), which is of a similar size to the iodide ion; this species effectively replaces the vacant site, thus restoring the full octahedral coordination of Pb.

These results suggest that adsorption and reduction of O_2 can effectively remove the trap states introduced by excess electrons and vacancies on the surface and in the bulk. The process will be rate limited by two general factors: (i) illumination that causes photoinduced migration of iodide ions down the illumination profile[18] leading to a gradient of additional iodide vacancies decreasing in density from the surface into the bulk, and (ii) diffusion of O_2 onto these surface and bulk iodide vacancies and the capture of an electron on these sites. Both of these factors may be responsible for the relatively slow PL rises observed in O_2 environments even in very low oxygen concentrations.[43] In particular, the dark grains are expected to have a larger starting density of vacancies than the bright grains, and are perhaps more susceptible to photoinduced vacancy generation; this would lead to lower initial PL levels but larger relative enhancements for the dark grains than the bright grains.

By contrast, the calculations suggest that H_2O adsorption does not cause any significant change in the surface electronic structure and unlikely to be responsible for the rapid baseline PL rise seen in the experiments in humid conditions. We conclude that the rapid baseline PL increase upon H_2O exposure for grains in both dark and light conditions is not due to an adsorption "defect-healing" process similar to that seen for O_2. Instead, we suggest that H_2O converts the surface region into a hydrate phase. Leguy et al.[44] have shown that this process of hydrate formation occurs very rapidly. The surface trap states would then be removed by such a conversion reaction, in which a very thin layer of the surface converts to an amorphous shell (of PbI_2 or PbO).[45] This shell eliminates the surface vacancies and explains the less reversible nature of the effects after exposure to humidity, particular humid air (cf. Figure 3).[21] We note that there is a very slow rise on top of the rapid baseline rise in humid conditions (Figure 1 b,c), which may be due to residual trace oxygen in the humidity source or the action of hydroxide ions in filling positively charged iodine vacancies.

For the case of N_2, the calculations suggest that it has little effect upon the surface electronic structure and the photoluminescence, due to it being unable to undergo either redox activity (like O_2) or promote conversion reactions (like H_2O). Nevertheless, the presence of adsorbed nitrogen molecules still gives more favorable conditions for luminescence than in vacuo in which the PL drops continually over time under illumination (cf. Figure S3, Supporting Information).

Finally, we note that the adsorption energies and density of states data for the (110) surface are very similar to the (001) surface (Figures S10–S15 and Table S2, Supporting Information). It has been reported that the crystal facets of $MAPbI_3$ can display different photovoltaic properties.[15] The data presented here suggest that the effectiveness of the treatment by atmospheric molecules will depend upon the intrinsic concentration of trap states present at a given facet. Finally, we note that here we are comparing in situ the luminescence of local grains in different environmental conditions under identical excitation conditions (e.g., pulse fluence, wavelength, and repetition rate). Future work will be required to explore the potentially large impact of these excitation parameters on the relative luminescence rise or decay in each atmosphere. Further future work should investigate whether the enhancements in the presence of atmospheric molecules and light can be maximized if selectively light-soaking defective grains or when light soaking the entire film.

In conclusion, we have used confocal photoluminescence measurements to show that the PL properties of $MAPbI_3$ perovskite grains under continual illumination depend sensitively on the type of grain (bright or dark) and type of adsorbed molecules. We find that dark grains show substantial enhancements under illumination in the presence of oxygen and/or water molecules, while bright grains show less of an effect. In nitrogen conditions, illumination leads to a net drop in PL over time, and this is further exaggerated in the absence of any molecules (in vacuo). We perform DFT calculations to show that oxygen, in the presence of photoexcited carriers, binds very strongly to iodide vacancies and reduces to superoxide. This removes the subgap electron trap states associated with the iodide vacancies, regenerating a band structure similar to the pristine case. We propose that moisture forms a thin passivating shell on the surfaces of the grains, in turn also eliminating the vacancies by converting the surfaces to benign amorphous species. In the absence of passivating molecules, continual illumination generates defects unabatedly. Our work provides a microscale view to resolve the seemingly conflicting literature in the field relating to the beneficial[18,19,21,23,26] and detrimental[31] effects of light soaking on the optoelectronic properties of perovskite films, and also provides crucial insights into the elimination of nonradiative decay in these exciting semiconductors. The work also suggests that future work should include searching for other molecules that could have similar passivating effects to O_2 and H_2O but do not lead to long-term degradation of the films.

Experimental Section

Photoluminescence Measurements: Confocal PL maps were acquired using a custom-built time-correlated single-photon counting confocal microscope (Nikon Eclipse Ti-E) setup with a 100X oil objective (Nikon CFI PlanApo Lambda, 1.45 NA). The samples were measured in the custom-built flow chamber with the desired gas and/or humidity level, where ultrahigh-purity dry gases (Airgas) were used and then controllably humidified. The cover slip samples were photoexcited through the glass-side using a 405 nm laser head (LDH-P-C-405, PicoQuant GmbH) with pulse duration of <90 ps, fluence of ≈1 µJ cm^{-2} per pulse, and a repetition rate of 0.5 MHz. The PL from the sample was collected by the same objective and the resulting collimated beam passes through a long-pass filter with a cut-off at 416 nm (Semrock Inc., BLP01-405R-25) to remove any residual scattered or reflected excitation light. A single photon detecting avalanche photodiode (MPD PDM Series 50 mm) was used for the detection. Light soaking was achieved

by directing the diffraction-limited pulsed laser spot onto a grain and collecting the emission for a period of time. The sample was scanned using a piezoelectric scanning stage. The measurements were acquired using the commercial software SymphoTime 64 (PicoQuant GmbH).

In vacuo measurements were acquired with the sample in a cryostat (Janis ST-100) at a pressure of <10^{-4} mbar. The samples were photoexcited with a 532 nm CW laser at intensities approximately equivalent to the photon fluxes of ≈2 sun irradiation (≈150 mW cm^{-2}). The PL was collected using fiber-coupled collecting optics and the emission detected using an Ocean Optics USB4000 fiber-coupled spectrometer.

Ab Initio Calculations: Density functional theory calculations were performed using the numeric atom-centered basis set all-electron code FHI-AIMS.[46,47] Light basis sets were used with tier 2 basis functions for C, N, H, and O. Electronic exchange and correlation were modeled with the semilocal Perdew–Burke–Ernzerhof (PBE) exchange-correlation functional.[48] A gamma point offset grid at a density of 0.04 Å^{-1} was used for k-point sampling. For the treatment of spin–orbit coupling, an atomic zeroth-order regular approximation[46] was used. Van der Waals forces were accounted for by applying a Tkatchenko–Sheffler electrodynamic screening scheme.[49] Molecules were adsorbed onto an eight layer surface slab of tetragonal MAPbI$_3$ containing 96 atoms with a vacuum gap of 20Å. Charged surfaces were compensated using the virtual crystal approximation.[50] Structures were relaxed with convergence criteria of 10^{-4} eV Å^{-1} for forces, 10^{-5} electrons for the electron density, and 10^{-7} eV for the total energy.

Supporting Information

Supporting Information is available online from the Wiley Online Library or from the author.

Conflict of Interest

The authors declare no conflict of interest.

[1] S. D. Stranks, H. J. Snaith, *Nat. Nanotechnol.* **2015**, *10*, 391.

[2] S. D. Stranks, P. K. Nayak, W. Zhang, T. Stergiopoulos, H. J. Snaith, *Angew. Chem.* **2015**, *54*, 3240.

[3] S. De Wolf, J. Holovsky, S.-J. Moon, P. Löper, B. Niesen, M. Ledinsky, F.-J. Haug, J.-H. Yum, C. Ballif, *J. Phys. Chem. Lett.* **2014**, *5*, 1035.

[4] a) S. D. Stranks, G. E. Eperon, G. Grancini, C. Menelaou, M. J. Alcocer, T. Leijtens, L. M. Herz, A. Petrozza, H. J. Snaith, *Science* **2013**, *342*, 341; b) L. M. Herz, *ACS Energy Lett.* **2017**, *2*, 1539.

[5] M. Saliba, T. Matsui, K. Domanski, J. Y. Seo, A. Ummadisingu, S. M. Zakeeruddin, J. P. Correa-Baena, W. R. Tress, A. Abate, A. Hagfeldt, M. Gratzel, *Science* **2016**, *354*, 206.

[6] W. S. Yang, B. W. Park, E. H. Jung, N. J. Jeon, Y. C. Kim, D. U. Lee, S. S. Shin, J. Seo, E. K. Kim, J. H. Noh, S. I. Seok, *Science* **2017**, *356*, 1376.

[7] a) Z. Xiao, R. A. Kerner, L. Zhao, N. L. Tran, K. M. Lee, T.-W. Koh, G. D. Scholes, B. P. Rand, *Nat. Photonics* **2017**, *11*, 108; b) N. Wang, L. Cheng, R. Ge, S. Zhang, Y. Miao, W. Zou, C. Yi, Y. Sun, Y. Cao, R. Yang, Y. Wei, Q. Guo, Y. Ke, M. Yu, Y. Jin, Y. Liu, Q. Ding, D. Di, L. Yang, G. Xing, H. Tian, C. Jin, F. Gao, R. H. Friend, J. Wang, W. Huang, *Nat. Photonics* **2016**, *10*, 699; c) H. Cho, S.-H. Jeong, M.-H. Park, Y.-H. Kim, C. Wolf, C.-L. Lee, J. H. Heo, A. Sadhanala, N. Myoung, S. Yoo, S. H. Im, R. H. Friend, T.-W. Lee, *Science* **2015**, *350*, 1222.

[8] B. R. Sutherland, E. H. Sargent, *Nat. Photonics* **2016**, *10*, 295.

[9] S. D. Stranks, *ACS Energy Lett.* **2017**, *2*, 1515.

[10] a) F. Deschler, M. Price, S. Pathak, L. E. Klintberg, D. D. Jarausch, R. Higler, S. Huttner, T. Leijtens, S. D. Stranks, H. J. Snaith, M. Atature, R. T. Phillips, R. H. Friend, *J. Phys. Chem. Lett.* **2014**, *5*, 1421; b) A. Baumann, S. Väth, P. Rieder, M. C. Heiber, K. Tvingstedt, V. Dyakonov, *J. Phys. Chem. Lett.* **2015**, *6*, 2350; c) M. L. Agiorgousis, Y.-Y. Sun, H. Zeng, S. Zhang, *J. Am. Chem. Soc.* **2014**, *136*, 14570.

[11] S. D. Stranks, V. M. Burlakov, T. Leijtens, J. M. Ball, A. Goriely, H. J. Snaith, *Phys. Rev. Appl.* **2014**, *2*, 034007.

[12] J. Nelson, *The Physics of Solar Cells*, Imperial College Press, London, UK **2003**.

[13] S. Draguta, S. Thakur, Y. V. Morozov, Y. Wang, J. S. Manser, P. V. Kamat, M. Kuno, *J. Phys. Chem. Lett.* **2016**, *7*, 715.

[14] D. W. deQuilettes, S. M. Vorpahl, S. D. Stranks, H. Nagaoka, G. E. Eperon, M. E. Ziffer, H. J. Snaith, D. S. Ginger, *Science* **2015**, *348*, 683.

[15] S. Y. Leblebici, L. Leppert, Y. Li, S. E. Reyes-Lillo, S. Wickenburg, E. Wong, J. Lee, M. Melli, D. Ziegler, D. K. Angell, D. F. Ogletree, Paul D. Ashby, F. M. Toma, J. B. Neaton, I. D. Sharp, A. Weber-Bargioni, *Nat. Energy* **2016**, *1*, 16093.

[16] a) Z. Zhao, X. Chen, H. Wu, X. Wu, G. Cao, *Adv. Funct. Mater.* **2016**, *26*, 3048; b) J. L. Garrett, E. M. Tennyson, M. Hu, J. Huang, J. N. Munday, M. S. Leite, *Nano Lett.* **2017**, *17*, 2554.

[17] O. D. Miller, E. Yablonovitch, S. R. Kurtz, *IEEE J. Photovoltaics* **2012**, *2*, 303.

[18] D. W. deQuilettes, W. Zhang, V. M. Burlakov, D. J. Graham, T. Leijtens, A. Osherov, V. Bulovic, H. J. Snaith, D. S. Ginger, S. D. Stranks, *Nat. Commun.* **2016**, *7*, 11683.

[19] Y. Tian, M. Peter, E. Unger, M. Abdellah, K. Zheng, T. Pullerits, A. Yartsev, V. Sundstrom, I. G. Scheblykin, *Phys. Chem. Chem. Phys.* **2015**, *17*, 24978.

[20] Y. Yamada, M. Endo, A. Wakamiya, Y. Kanemitsu, *J. Phys. Chem. Lett.* **2015**, *6*, 482.

[21] R. Brenes, D. Guo, A. Osherov, N. K. Noel, C. Eames, E. M. Hutter, S. K. Pathak, F. Niroui, R. H. Friend, M. S. Islam, H. J. Snaith, V. Bulović, T. J. Savenije, S. D. Stranks, *Joule* **2017**, *1*, 155.

[22] E. Mosconi, D. Meggiolaro, H. J. Snaith, S. D. Stranks, F. De Angelis, *Energy Environ. Sci.* **2016**, *9*, 3180.

[23] J. F. Galisteo-López, M. Anaya, M. E. Calvo, H. Míguez, *J. Phys. Chem. Lett.* **2015**, *6*, 2200.

[24] a) M. L. Petrus, Y. Hu, D. Moia, P. Calado, A. M. A. Leguy, P. R. F. Barnes, P. Docampo, *ChemSusChem* **2016**, *9*, 2699; b) C. Müller, T. Glaser, M. Plogmeyer, M. Sendner, S. Döring, A. A. Bakulin, C. Brzuska, R. Scheer, M. S. Pshenichnikov, W. Kowalsky, A. Pucci, R. Lovrin ić, *Chem. Mater.* **2015**, *27*, 7835;

ADVANCED
SCIENCE NEWS

www.advancedsciencenews.com

ADVANCED
MATERIALS

www.advmat.de

c) J. You, Y. Yang, Z. Hong, T.-B. Song, L. Meng, Y. Liu, C. Jiang, H. Zhou, W.-H. Chang, G. Li, Y. Yang, *Appl. Phys. Lett.* **2014**, *105*, 183902.

[25] G. E. Eperon, S. N. Habisreutinger, T. Leijtens, B. J. Bruijnaers, J. J. van Franeker, D. W. deQuilettes, S. Pathak, R. J. Sutton, G. Grancini, D. S. Ginger, R. A. Janssen, A. Petrozza, H. J. Snaith, *ACS Nano* **2015**, *9*, 9380.

[26] H.-H. Fang, S. Adjokatse, H. Wei, J. Yang, G. R. Blake, J. Huang, J. Even, M. A. Loi, *Sci. Adv.* **2016**, *2*, e1600534.

[27] G. Grancini, V. D'Innocenzo, E. R. Dohner, N. Martino, A. R. Srimath Kandada, E. Mosconi, F. De Angelis, H. I. Karunadasa, E. T. Hoke, A. Petrozza, *Chem. Sci.* **2015**, *6*, 7305.

[28] N. Aristidou, I. Sanchez-Molina, T. Chotchuangchutchaval, M. Brown, L. Martinez, T. Rath, S. A. Haque, *Angew. Chem., Int. Ed.* **2015**, *54*, 8208.

[29] N. Aristidou, C. Eames, I. Sanchez-Molina, X. Bu, J. Kosco, M. S. Islam, S. A. Haque, *Nat. Commun.* **2017**, *8*, 15218.

[30] T. Leijtens, G. E. Eperon, N. K. Noel, S. N. Habisreutinger, A. Petrozza, H. J. Snaith, *Adv. Energy Mater.* **2015**, *5*, 1500962.

[31] a) R. Gottesman, L. Gouda, B. S. Kalanoor, E. Haltzi, S. Tirosh, E. Rosh-Hodesh, Y. Tischler, A. Zaban, C. Quarti, E. Mosconi, F. De Angelis, *J. Phys. Chem. Lett.* **2015**, *6*, 2332; b) W. Nie, J.-C. Blancon, A. J. Neukirch, K. Appavoo, H. Tsai, M. Chhowalla, M. A. Alam, M. Y. Sfeir, C. Katan, J. Even, S. Tretiak, J. J. Crochet, G. Gupta, A. D. Mohite, *Nat. Commun.* **2016**, *7*, 11574.

[32] W. Zhang, S. Pathak, N. Sakai, T. Stergiopoulos, P. K. Nayak, N. K. Noel, A. A. Haghighirad, V. M. Burlakov, D. W. deQuilettes, A. Sadhanala, W. Li, L. Wang, D. S. Ginger, R. H. Friend, H. J. Snaith, *Nat. Commun.* **2015**, *6*, 10030.

[33] M. Yang, Y. Zeng, Z. Li, D. H. Kim, C.-S. Jiang, J. van de Lagemaat, K. Zhu, *Phys. Chem. Chem. Phys.* **2017**, *19*, 5043.

[34] J. Haruyama, K. Sodeyama, L. Han, Y. Tateyama, *Acc. Chem. Res.* **2016**, *49*, 554.

[35] L. She, M. Liu, D. Zhong, *ACS Nano* **2016**, *10*, 1126.

[36] a) A. Ng, Z. Ren, Q. Shen, S. H. Cheung, H. C. Gokkaya, S. K. So, A. B. Djurišić, Y. Wan, X. Wu, C. Surya, *ACS Appl. Mater. Interfaces* **2016**, *8*, 32805; b) W. Hao, X. Chen, S. Li, *J. Phys. Chem. C* **2016**, *120*, 28448; c) E. Mosconi, J. M. Azpiroz, F. De Angelis, *Chem. Mater.* **2015**, *27*, 4885; d) G. Gordillo, C. A. Otalora, A. A. Ramirez, *Phys. Chem. Chem. Phys.* **2016**, *18*, 32862.

[37] N. Z. Koocher, D. Saldana-Greco, F. Wang, S. Liu, A. M. Rappe, *J. Phys. Chem. Lett.* **2015**, *6*, 4371.

[38] L. Zhang, P. H. L. Sit, *J. Mater. Chem. A* **2017**, *5*, 9042.

[39] R. I. Masel, *Principles of Adsorption and Reaction on Solid Surfaces*, John Wiley & Sons, New York **1996**.

[40] a) M. Bowker, *The Basis and Applications of Heterogeneous Catalysis*, Oxford University Press, New York **1998**; b) G. C. Bond, *Heterogeneous Catalysis*, Oxford University Press, Oxford, UK **1987**.

[41] H. Uratani, K. Yamashita, *J. Phys. Chem. Lett.* **2017**, *8*, 742.

[42] a) M.-H. Du, *J. Phys. Chem. Lett.* **2015**, *6*, 1461; b) A. Buin, R. Comin, J. Xu, A. H. Ip, E. H. Sargent, *Chem. Mater.* **2015**, *27*, 4405.

[43] S. G. Motti, M. Gandini, A. J. Barker, J. M. Ball, A. R. Srimath Kandada, A. Petrozza, *ACS Energy Lett.* **2016**, *1*, 726.

[44] A. M. A. Leguy, Y. Hu, M. Campoy-Quiles, M. I. Alonso, O. J. Weber, P. Azarhoosh, M. van Schilfgaarde, M. T. Weller, T. Bein, J. Nelson, P. Docampo, P. R. F. Barnes, *Chem. Mater.* **2015**, *27*, 3397.

[45] Q. Chen, H. Zhou, T. B. Song, S. Luo, Z. Hong, H. S. Duan, L. Dou, Y. Liu, Y. Yang, *Nano Lett.* **2014**, *14*, 4158.

[46] V. Blum, R. Gehrke, F. Hanke, P. Havu, V. Havu, X. Ren, K. Reuter, M. Scheffler, *Comput. Phys. Commun.* **2009**, *180*, 2175.

[47] R. Xinguo, R. Patrick, B. Volker, W. Jürgen, T. Alexandre, S. Andrea, R. Karsten, S. Matthias, *New J. Phys.* **2012**, *14*, 053020.

[48] J. P. Perdew, K. Burke, M. Ernzerhof, *Phys. Rev. Lett.* **1996**, *77*, 3865.

[49] N. A. Richter, S. Sicolo, S. V. Levchenko, J. Sauer, M. Scheffler, *J. Chem. Phys.* **2013**, *138*, 074106.

[50] N. A. Richter, S. Sicolo, S. V. Levchenko, J. Sauer, M. Scheffler, *Phys. Rev. Lett.* **2013**, *111*, 045502.